

## BOUNDEDNESS, STABILITY AND PATTERN FORMATION FOR A PREDATOR-PREY MODEL WITH SIGMOID FUNCTIONAL RESPONSE AND PREY-TAXIS

ZHIHONG ZHAO, HUANQIN HU

**ABSTRACT.** This article concerns the structure of the nonconstant steady states for a predator-prey model of Leslie-Gower type with Sigmoid functional and prey-taxis subject to the homogeneous Neumann boundary condition. The existence of bounded classical global solutions is discussed in bounded domains with arbitrary spatial dimension and any prey-taxis sensitivity coefficient. The local stability of the homogeneous steady state is analyzed to show that the prey-taxis sensitivity coefficient destabilizes the stability of the homogeneous steady state when prey defends. Then we study the existence and stability of the nonconstant positive steady state of the system over 1D domain by applying the bifurcation theory and present properties of local branches such as pitchfork and turning direction. Moreover, we discuss global bifurcation, homogeneous steady state solutions, nonconstant steady states solutions, spatio-temporal periodic solutions and spatio-temporal irregular solutions which demonstrate the coexistence and spatial distribution of prey and predator species. Finally, we perform numerical simulations to illustrate and support our theoretical analysis.

### 1. INTRODUCTION

In the field of biomathematics, the study of predator-prey interactions is one of the fundamental subject. It is well known that there are a large number of factors that influence dynamics of the predator-prey models, such as the birth rate, mortality, interspecific competition, food, infectious disease, and functional responses etc. One of the typical functional responses is the Holling II type:

$$P(u) = \frac{bu}{bhu + 1},$$

where  $u$  is the density of the prey, the positive constants  $b$  and  $h$  denote the search rate and the processing time, respectively. It applies to invertebrates [19] (insects and parasitic species are included here) and can be seen that the predator search rate  $b$  is constant. As the study progressed, Hessel [8] pointed out that many invertebrate predators search actively when the density of prey increases, and that the search efficiency of predators decreases when density of prey falls below a certain threshold, e.g., *Coccinella septempunctata* and first instar aphid, *Plea atomaria* and

---

2020 *Mathematics Subject Classification.* 35B32, 35J67, 35K57, 92D25, 92D40.

*Key words and phrases.* Predator-prey model; prey-taxis; boundedness; steady states; global bifurcation; pattern formation.

©2023. This work is licensed under a CC BY 4.0 license.

Submitted January 6, 2023. Published May 4, 2023.

small *Aedes* larvae. This means that the search rate of many invertebrate predators depends on the density of prey, i.e.,  $b = \frac{au}{u+g}$ , where the positive constants  $a$  and  $g$  denote the maximum achievable search rate and the half-saturation constant, respectively. In this way we obtain the Sigmoid functional response [6], which is the so-called generalized Holling type III:

$$P(u) = \frac{au^2}{ahu^2 + u + g}. \quad (1.1)$$

Turing [29] proposed a reaction diffusion system for the chemical basis of morphogenesis, which is one of the most important mechanisms in theoretical biology. Since the spatial heterogeneity of the environment affects predator-prey dynamics, such system has been extensively investigated since 1970s. In particular, Turing bifurcation, Hopf bifurcation, pattern formation and traveling wave have been widely studied [10, 25, 26, 28, 31, 32], where spatial diffusion refers to the variation of species density according to some process (e.g., physical diffusion or random walk diffusion).

Kareiva and Odell [13] pointed out that predators move toward areas of high prey density to improve predation efficiency when the area is restricted, creating a predator aggregation phenomenon. This behavior can be considered as the movement of the predators in the direction of the prey density gradient, which is called prey-taxis. Moreover, the predator-prey model with prey-taxis is different from the previous models and has rich spatial-temporal dynamics. Global existence, bifurcation analysis and pattern formation of prey-taxis systems have been widely studied [2, 9, 16, 20, 24, 27, 33, 34, 36, 37, 38, 39] and the references therein.

In this article, we consider a predator-prey system with prey-taxis:

$$\begin{aligned} \frac{\partial u}{\partial t} &= d_1 \Delta u + ru \left(1 - \frac{u}{K}\right) - P(u)v, & \text{in } (0, T) \times \Omega, \\ \frac{\partial v}{\partial t} &= d_2 \Delta v - \xi \nabla(\chi(v) \nabla u) + sv \left(1 - e \frac{v}{u}\right), & \text{in } (0, T) \times \Omega, \\ \frac{\partial u}{\partial \nu} &= \frac{\partial v}{\partial \nu} = 0, & \text{on } (0, T) \times \partial \Omega, \\ u(x, 0) &= u_0(x) \geq 0, \quad v(x, 0) = v_0(x) \geq 0, & \text{in } \Omega, \end{aligned} \quad (1.2)$$

where  $u(x, t)$ ,  $v(x, t)$  are the density of the prey and predator at position  $x$  and time  $t$  respectively, the habitat of both species  $\Omega$  is a bounded domain with a smooth boundary  $\partial \Omega$  in  $\mathbb{R}^n$  ( $n \geq 1$  is a positive integer),  $\nu$  is the outward unit normal vector of the boundary  $\partial \Omega$ , the initial data  $u_0(x)$ ,  $v_0(x)$  are nonnegative continuous functions and the positive constants  $d_1, d_2$  are diffusion coefficients. The parameters  $r$  and  $s$  represent the intrinsic growth rate. The prey population grows logistically with the carrying capacity  $K$ . The predator consumes the prey according to the sigmoid functional response  $P(u)$ . The term  $\frac{ev}{u}$  is known as the Leslie-Gower term [17, 18], and  $e$  is the number of prey required to support one predator when  $v$  equals  $\frac{u}{e}$ . The parameter  $\xi$  denotes the prey-taxis sensitivity coefficient,  $\chi(v)$  denotes the prey-tactic cross diffusion and the term  $\xi \chi(v) \nabla u$  denotes the speed of the predator moving in the direction of the density gradient of the prey. For the prey-taxis sensitivity coefficient  $\xi$ ,  $\xi > 0$  indicates that the predator moves in the direction of high prey density to improve predation efficiency, and  $\xi < 0$  indicates that the predator moves in the opposite direction of high prey density in order to avoid the group defense of large amounts of prey, which is exemplified in nature by Japanese

bees that gather together to form a hot ball to kill bumblebees when faced with bumblebees [3, 15]. More biological background can be found in [12, 30].

For convenience, we dimensionless size the model (1.2) as

$$\begin{aligned} \bar{u} &= \frac{u}{K}, \quad \bar{t} = rt, \quad \bar{d}_1 = \frac{d_1}{r}, \quad \bar{a} = Kah, \quad \bar{g} = \frac{g}{K}, \quad \bar{u}_0 = \frac{u_0}{K}, \quad \bar{v} = \frac{av}{r} \\ \bar{d}_2 &= \frac{d_2}{r}, \quad \bar{\xi} = \frac{aK\xi}{r^2}, \quad \bar{\chi}(\bar{v}) = \chi(v), \quad \bar{c} = \frac{s}{r}, \quad \bar{\delta} = \frac{re}{aK}, \quad \bar{v}_0 = \frac{av_0}{r}, \end{aligned}$$

and ignore the bars on  $u$ ,  $v$  and other parameters, then system (1.2) can be re-expressed by

$$\begin{aligned} \frac{\partial u}{\partial t} &= d_1 \Delta u + u(1-u) - \frac{u^2 v}{au^2 + u + g}, \quad \text{in } (0, T) \times \Omega, \\ \frac{\partial v}{\partial t} &= d_2 \Delta v - \xi \nabla(\chi(v) \nabla u) + cv(1 - \frac{v}{\delta u}), \quad \text{in } (0, T) \times \Omega, \\ \frac{\partial u}{\partial \nu} &= \frac{\partial v}{\partial \nu} = 0, \quad \text{on } (0, T) \times \partial\Omega, \\ u(x, 0) &= u_0(x) \geq 0, v(x, 0) = v_0(x) \geq 0, \quad \text{in } \Omega. \end{aligned} \tag{1.3}$$

Throughout this paper we assume that

(H1)  $\chi(v) \in C^4[0, \infty)$ ,  $\chi(0) = 0$  and there exists  $B > 0$  such that  $\chi(v) \leq Bv$  for any  $v \geq 0$  and  $x \in \bar{\Omega}$ .

In this article, we investigate the global existence of the classical solution and the effect of the prey-taxis sensitivity coefficient on the stability, non-constant positive steady state and pattern formation of (1.3). Main results reveal that system (1.3) has global bounded classical solutions in bounded domains, the prey-taxis destabilizes the stability of the homogeneous steady state in the corresponding ODE system or the PDE system with random diffusion, and a nonconstant positive steady-state bifurcation occurs at the critical bifurcation point. Numerical simulations are carried out to verify our theoretical results. We also find that the period of the spatio-temporal periodic solutions becomes greater when the intrinsic growth rate of predators increases within a certain range, which is a novel outcome of this study.

The rest part of this paper is organized as follows. In Section 2, we prove the global existence and boundedness of the classical solution. In Section 3, we perform the stability of the homogeneous steady state by linearizing the model. Section 4 is devoted to establishing the existence of a non-constant positive steady state in one-dimensional space, the stability of this steady branch and the global bifurcation. In Section 5, numerical simulations are presented. We discuss our results and raise some interesting problems for the future study.

**1.1. Global solutions.** In this section, we discuss the existence of global solutions of the initial-boundary value problem (1.3) of arbitrary spatial dimension with any prey-taxis sensitivity coefficient.

**Theorem 1.1.** *If  $u_0(x) > 0$ ,  $v_0(x) \geq 0$ , then the system (1.3) admits a unique classical solution  $(u(x, t), v(x, t))$  for all  $x \in \Omega, t > 0$ . Furthermore, there exist constants  $U_i > 0$ ,  $V_i \geq 0$ ,  $i = 1, 2$  depending on the initial values  $u_0(x)$  and  $v_0(x)$  such that*

$$U_1 < u(x, t) < U_2, \quad V_1 < v(x, t) < V_2, \quad x \in \Omega, \quad t > 0.$$

*Proof.* The existence and uniqueness of the solution to the initial-boundary value problem (1.3) is easily obtained. For the global existence and the boundedness, we apply the theory of invariant region in [35]. For the vector field

$$\left(u(1-u) - \frac{u^2v}{au^2+u+g}, cv\left(1 - \frac{v}{\delta u}\right)\right),$$

if there exists a region  $\mathfrak{R} = (U_1, U_2) \times (V_1, V_2)$  in the  $(u, v)$  phase plane such that the vector field points inward on the boundary of  $\mathfrak{R}$ , then  $\mathfrak{R}$  is a (positively) invariant rectangle. If  $\mathfrak{R}$  is positively invariant to the vector field then the solution exists globally and is bounded.

Let

$$U_2 = \max \left\{1, \max_{x \in \bar{\Omega}} u_0(x)\right\}, \quad V_2 = \max \left\{\delta, \max_{x \in \bar{\Omega}} v_0(x)\right\},$$

$$U_1 = \min \left\{\frac{g}{g+\delta}, \min_{x \in \bar{\Omega}} u_0(x)\right\}, \quad V_1 = \min \left\{0, \min_{x \in \bar{\Omega}} v_0(x)\right\}.$$

Clearly, the initial functions  $u_0(x)$  and  $v_0(x)$  are enclosed by the rectangle. And for  $u = U_1, V_1 \leq v \leq V_2$ , we have

$$u(1-u) - \frac{u^2v}{au^2+u+g} \geq U_1(1-U_1) - \frac{U_1^2\delta}{g} \geq 0,$$

which means that the vector field crosses this line in the direction pointing to the interior of  $\mathfrak{R}$ . For the other three sides, we verify using similar calculations.

Therefore, the region  $\mathfrak{R}$  is positively invariant with respect to the vector field and the the proof is complete.  $\square$

## 2. STABILITY ANALYSIS OF HOMOGENEOUS STEADY STATE

In this section, we analyze the stability of the nontrivial homogeneous steady state  $(u^*, v^*)$  by the characteristic equations. It can be seen that the corresponding ODE system of system (1.3) is a predator-prey model of Leslie-Gower type with Sigmoid functional response. Huang [11] investigated the types of equilibrium and bifurcations of this ODE system for different values of parameters. By simple calculation, system (1.3) has a boundary equilibrium  $(1, 0)$  and unique interior equilibrium  $(u^*, v^*)$ , where  $u^*$  satisfies:

$$h(u) = au^3 + (\delta + 1 - a)u^2 + (g - 1)u - g = 0 \quad (2.1)$$

and  $v^* = \delta u^*$ . It is clear that  $h(0) = -g < 0$ ,  $h(1) = \delta > 0$ , then  $u^* \in (0, 1)$ . By Cardano's Method, (2.1) has a unique positive solution  $u^*$ ,

$$u^* = \sqrt[3]{-\frac{q}{2} + \sqrt{\Delta}} + \sqrt[3]{-\frac{q}{2} - \sqrt{\Delta}} - \frac{\delta + 1 - a}{3a},$$

when  $\Delta = \left(\frac{q}{2}\right)^2 - \left(\frac{p}{3}\right)^3 > 0$ , where

$$p = \frac{3a(g-1) - (\delta+1-a)^2}{3a^2}, \quad q = \frac{2(\delta+1-a)^3 - 27a^2g - 9a(\delta+1-a)(g-1)}{27a^3}.$$

We make the following assumption:

(H2)  $\Delta > 0$  and

$$1 - 2u^* - \frac{(1-u^*)^2(u^*+2g)}{\delta u^{*2}} < c.$$

And let

$$f(u, v) = u(1 - u) - \frac{u^2v}{au^2 + u + g}, \quad g(u, v) = cv(1 - \frac{v}{\delta u}).$$

then we have the following results for the stability of the homogeneous steady state  $(u^*, v^*)$  for ODE system.

**Lemma 2.1.** *If (H2) holds, then the homogeneous steady state  $(u^*, v^*)$  is locally asymptotically stable for system (1.3) without spatial variation.*

*Proof.* Linearizing (1.3) without spatial variation at the steady state  $(u^*, v^*)$ , then we obtain  $U_t = AU$ , where

$$U = \begin{pmatrix} u \\ v \end{pmatrix}, \quad A = \begin{pmatrix} f_1 & f_2 \\ g_1 & g_2 \end{pmatrix}, \tag{2.2}$$

and

$$f_1 = f_u(u^*, v^*) = 1 - 2u^* - \frac{(1 - u^*)^2(u^* + 2g)}{\delta u^{*2}}, \quad f_2 = f_v(u^*, v^*) = \frac{u^* - 1}{\delta} < 0,$$

$$g_1 = g_u(u^*, v^*) = c\delta > 0, \quad g_2 = g_v(u^*, v^*) = -c < 0.$$

Clearly,  $f_1g_2 - f_2g_1 > 0$ , thus the locally asymptotically stability of  $(u^*, v^*)$  can be guaranteed when  $f_1 + g_2 = 1 - 2u^* - \frac{(1 - u^*)^2(u^* + 2g)}{\delta u^{*2}} - c < 0$  holds.  $\square$

Before developing our argument, let us set up the following notation.

- $0 = \sigma_0 < \sigma_1 < \sigma_2 < \dots$  are the eigenvalues for the elliptic operator  $-\Delta$  on  $\Omega$  under the homogeneous Neumann boundary condition.
- $E(\sigma_i)$  and  $\phi_{ij}, j = 1, 2, \dots, \dim E(\sigma_i)$  be the eigenspace and eigenfunctions corresponding to eigenvalue  $\sigma_i, i = 0, 1, 2, \dots$ , respectively.
- $\mathbf{X}_{ij} := \{c \cdot \phi_{ij}, c \in \mathbb{R}^2\}$ , where  $\{\phi_{ij}\}$  are standard orthogonal bases in space  $E(\sigma_i)$ , for  $j = 1, 2, \dots, \dim E(\sigma_i)$ .
- $\mathbf{X} := [L^2(\Omega)]^2$ , then  $\mathbf{X} = \bigoplus_{i=1}^{+\infty} \mathbf{X}_i$  and  $\mathbf{X}_i = \bigoplus_{j=1}^{\dim E(\sigma_i)} \mathbf{X}_{ij}$ .

Then the stability of  $(u^*, v^*)$  of system (1.3) is given in the following theorem.

**Theorem 2.2.** *Assume (H2) holds, and denote*

$$Q_i(\sigma_i, 0) = d_1d_2\sigma_i^2 - (d_1g_2 + d_2f_1)\sigma_i + f_1g_2 - f_2g_1, \quad i \geq 1, \tag{2.3}$$

$$\xi_i := \frac{Q_i(\sigma_i, 0)}{\chi(v^*)f_2\sigma_i}, i \geq 1 \quad \text{and} \quad \hat{\xi} := \max_{1 \leq i \leq \infty} \xi_i. \tag{2.4}$$

*Then the homogeneous steady state  $(u^*, v^*)$  is locally asymptotically stable for any  $\xi > \hat{\xi}$  and  $(u^*, v^*)$  is unstable when  $\xi < \hat{\xi}$ .*

*Proof.* Linearizing system (1.3) at  $(u^*, v^*)$ , we obtain

$$U_t = (A + D\Delta)U, \quad D = \begin{pmatrix} d_1 & 0 \\ -\xi\chi(v^*) & d_2 \end{pmatrix}, \tag{2.5}$$

where  $A$  and  $U$  are the same as (2.2). Assume that  $(\varphi, \psi)$  is the eigenfunction corresponding to the eigenvalue  $\mu$  of operator  $A + D\Delta$ , then they can be expressed as

$$\begin{pmatrix} \varphi \\ \psi \end{pmatrix} = \sum_{0 \leq i < \infty, 1 \leq j \leq \dim E(\sigma_i)} \begin{pmatrix} a_{ij} \\ b_{ij} \end{pmatrix} \phi_{ij}(x). \tag{2.6}$$

And the characteristic equation of (2.5) for an eigenvalue is

$$\mu^2 - P_i(\sigma_i)\mu + Q_i(\sigma_i, \xi) = 0,$$

where  $P_i(\sigma_i) = -(d_1 + d_2)\sigma_i + f_1 + g_2 < 0$  and  $Q_i(\sigma_i, \xi) = d_1d_2\sigma_i^2 - (\xi\chi(v^*)f_2 + d_2f_1 + d_1g_2)\sigma_i + f_1g_2 - f_2g_1, i \geq 1$ . By (2.3), we have

$$Q_i(\sigma_i, \xi) = Q_i(\sigma_i, 0) - \xi\chi(v^*)f_2\sigma_i. \quad (2.7)$$

It is easy to obtain that  $(u^*, v^*)$  is local asymptotic stability by  $Q_i(0, \xi) = f_1g_2 - f_2g_1 > 0$  if  $i = 0$ . For  $i \geq 1$ , we have:

- (i)  $Q_i(\sigma_i, 0) > 0$  for all  $i \geq 1$ . Then  $\hat{\xi} < 0$  by (2.4). If  $\xi > \hat{\xi}$ , then  $Q_i(\sigma_i, 0) - \xi\chi(v^*)f_2\sigma_i > Q_i(\sigma_i, 0) - \hat{\xi}\chi(v^*)f_2\sigma_i = 0$  for every  $i$ , which implies  $(u^*, v^*)$  is local asymptotically stable by (2.7). If  $\xi < \hat{\xi}$ , then  $Q_i(\sigma_i, 0) - \xi\chi(v^*)f_2\sigma_i < 0$  for some  $i$ , which means  $(u^*, v^*)$  is unstable.
- (ii)  $Q_i(\sigma_i, 0) < 0$  for some  $i \geq 1$ . Then  $\hat{\xi} > 0$  by (2.4). If  $\xi > \hat{\xi}$ , then  $Q_i(\sigma_i, 0) - \xi\chi(v^*)f_2\sigma_i > Q_i(\sigma_i, 0) - \hat{\xi}\chi(v^*)f_2\sigma_i = 0$  for every  $i$ . Thus,  $(u^*, v^*)$  is local asymptotically stable by (2.7). If  $\xi < \hat{\xi}$ , then  $Q_i(\sigma_i, 0) - \xi\chi(v^*)f_2\sigma_i < 0$  for some  $i$ . Thus  $(u^*, v^*)$  is unstable.

□

From Theorem 2.2, we can point out that the homogeneous steady state  $(u^*, v^*)$  loses its stability when prey-taxis sensitivity coefficient is less than a certain threshold value  $\hat{\xi}$ . In what follows, we only discuss case (i):  $Q_i(\sigma_i, 0) > 0$  for all  $i \geq 1$  in the proof of Theorem 2.2 while case (ii) can be treated by the same arguments.

### 3. NONCONSTANT POSITIVE STEADY STATES

In this section, we study the existence, stability and global bifurcation analysis of the nonconstant steady states to model (1.3) in the 1D interval  $(0, l)$ ,  $l > 0$  with prey-taxis sensitivity coefficient  $\xi < \hat{\xi}$ . The eigenvalues of  $-\Delta$  on  $(0, l)$  under homogeneous Neumann boundary condition are  $\sigma_i = (\frac{i\pi}{l})^2, i = 0, 1, 2, \dots$ , and the corresponding eigenfunctions are  $\phi_i = \cos(\frac{i\pi x}{l}), i = 0, 1, 2, \dots$ .

**3.1. Existence of nonconstant steady states.** In this part, we apply Crandall-Rabinowitz bifurcation theory [4] with  $\xi$  as the bifurcation parameter to show that the system (1.3) can generate a branch of nonconstant steady state solutions, which bifurcate from the homogeneous steady state  $(u^*, v^*)$ . To be precise, we consider the corresponding strongly coupled elliptic system of model (1.3):

$$\begin{aligned} d_1\Delta u + u(1-u) - \frac{u^2v}{au^2+u+g} &= 0, & x \in (0, l), \\ d_2\Delta v - \xi\nabla(\chi(v)\nabla u) + cv(1 - \frac{v}{\delta u}) &= 0, & x \in (0, l), \\ u' = v' = 0, & & x = 0, l. \end{aligned} \quad (3.1)$$

Then (3.1) can be expressed as

$$F(\xi, u, v) = 0, \quad (\xi, u, v) \in \mathbb{R} \times \mathcal{X},$$

where

$$F(\xi, u, v) = \left( \begin{array}{c} d_1\Delta u + u(1-u) - \frac{u^2v}{au^2+u+g} \\ d_2\Delta v - \xi\nabla(\chi(v)\nabla u) + cv(1 - \frac{v}{\delta u}) \end{array} \right),$$

$$\mathcal{X} = \{(u, v) : u, v \in H^2([0, l]), u' = v' = 0 \text{ at } x = 0, l\}.$$

It is obvious that the solution of  $F = 0$  is the classical solution of (3.1), and  $F$  is a continuously differentiable mapping from  $\mathbb{R} \times \mathcal{X}$  to  $\mathcal{Y}$ ,  $\mathcal{Y} = L^2(0, l) \times L^2(0, l)$ . Moreover,  $F(\xi, u^*, v^*) = 0$  for any  $\xi \in \mathbb{R}$ .

If  $(\alpha, u^*, v^*)$  is a bifurcation point of  $F = 0$  with respect to the curve  $(\xi, u^*, v^*)$ , then the solution of  $F = 0$  not lying on this curve in any neighbourhood of  $(\alpha, u^*, v^*)$ . Base on (2.4) and (2.7), the derivative operator

$$F_{(u,v)}(\xi, u^*, v^*) = \begin{pmatrix} d_1\Delta + f_1 & f_2 \\ g_1 - \xi\chi(v^*)\Delta & d_2\Delta + g_2 \end{pmatrix}$$

satisfies

$$(A + D\Delta)(\xi_i) = F_{(u,v)}(\xi_i, u^*, v^*) \tag{3.2}$$

and  $Q_i(\sigma_i, \xi_i) = 0$  by Theorem 2.2. Therefore,  $F_{(u,v)}(\xi_i, u^*, v^*)$  has zero eigenvalue, which implies that  $(\xi_i, u^*, v^*)$  may be bifurcation points for all  $i \geq 1$  as follow. We now show that the local bifurcation does occur at  $(\xi_i, u^*, v^*)$  for all  $i \geq 1$ .

**Theorem 3.1.** *Assuming (H2) holds, and  $\xi_i \neq \xi_k$  for any  $k \neq i$ , then  $(\xi_i, u^*, v^*)$  is a bifurcation point with respect to the curve  $(\xi, u^*, v^*)$ , where  $\xi_i$  is defined in (2.4). That is there exists a constant  $\delta > 0$  such that for each positive integer  $i$ , system (3.1) has non-constant positive solutions  $\Gamma_i(s) = (\xi_i(s), u_i(s, x), v_i(s, x))$  for  $|s| < \delta$ , where  $\xi_i(s) \in \mathbb{R}$  and  $(u_i(s, x), v_i(s, x)) \in \mathcal{X}$  are smooth function of  $s$ . Furthermore,  $\Gamma_i(s)$  around  $(\xi_i, u^*, v^*)$  can be expressed as*

$$\begin{aligned} (u_i(s, x), v_i(s, x)) &= (u^*, v^*) + s(1, b_i) \cos \frac{i\pi x}{l} + o(s), \\ \xi_i(s) &= \xi_i + sK_1 + s^2K_2 + \dots, \end{aligned} \tag{3.3}$$

where  $b_i = \frac{d_1\sigma_i - f_1}{f_2}$ ,  $K_1, K_2$  are constants to be determined and

$$\begin{aligned} (u_i(s, x), v_i(s, x)) - (u^*, v^*) - s(1, b_i) \cos \frac{i\pi x}{l} \\ \in \left\{ (u, v) \in \mathcal{X} : \int_0^1 (u\hat{u}_i + v\hat{v}_i)dx = 0 \right\} \equiv \mathcal{Z}, \end{aligned}$$

where  $(\hat{u}_i, \hat{v}_i) = (1, b_i) \cos \frac{i\pi x}{l}$ .

*Proof.* For fixed  $i$ , we only need to prove the following conditions hold by [4, Theorem 1.7].

- (1) The partial derivatives  $F_\xi, F_{(u,v)}$  and  $F_{(\xi,u,v)}$  exist and are continuous;
- (2)  $\dim \mathcal{N}(F_{(u,v)}(\xi_i, u^*, v^*)) = \dim \mathcal{Y} / \mathcal{R}(F_{(u,v)}(\xi_i, u^*, v^*)) = 1$ ,
- (3)  $\mathcal{N}(F_{(u,v)}(\xi_i, u^*, v^*)) = \text{span} \{(\hat{u}_i, \hat{v}_i)\}$  and

$$F_{(\xi,u,v)}(\xi_i, u^*, v^*)(\hat{u}_i, \hat{v}_i) \notin \mathcal{R}(F_{(u,v)}(\xi_i, u^*, v^*)).$$

From calculations, we obtain

$$\begin{aligned} F_\xi(\xi, u, v) &= - \begin{pmatrix} 0 \\ \nabla(\chi(v)\nabla u) \end{pmatrix}, \\ F_{(\xi,u,v)}(\xi, u, v)(p, q) &= - \begin{pmatrix} 0 \\ \nabla(\chi(v)\nabla p) + \nabla(\chi'(v)q\nabla u) \end{pmatrix} \end{aligned} \tag{3.4}$$

Clearly,  $F_\xi, F_{(u,v)}$  and  $F_{(\xi,u,v)}$  are continuous. Let

$$\begin{pmatrix} \varphi \\ \psi \end{pmatrix} = \sum_{0 \leq i < \infty} \begin{pmatrix} a_i \\ b_i \end{pmatrix} \cos \frac{i\pi x}{l} \in \mathcal{N}(F_{(u,v)}(\xi_i, u^*, v^*)).$$

Then

$$\sum_{0 \leq i < \infty} \begin{pmatrix} d_1 \Delta + f_1 & f_2 \\ g_1 - \xi_i \chi(v^*) \Delta & d_2 \Delta + g_2 \end{pmatrix} \begin{pmatrix} a_i \\ b_i \end{pmatrix} \cos \frac{i\pi x}{l} = 0, \quad (3.5)$$

and therefore the coefficient matrix in (3.5) is singular, that is,

$$\det \begin{pmatrix} d_1 \Delta + f_1 & f_2 \\ g_1 - \xi_i \chi(v^*) \Delta & d_2 \Delta + g_2 \end{pmatrix} = \det \begin{pmatrix} -d_1 \sigma_i + f_1 & f_2 \\ g_1 + \xi_i \chi(v^*) \sigma_i & -d_2 \sigma_i + g_2 \end{pmatrix} = 0, \quad (3.6)$$

which implies

$$\begin{aligned} \dim \mathcal{N}(F_{(u,v)}(\xi_i, u^*, v^*)) &= 1, \\ \mathcal{N}(F_{(u,v)}(\xi_i, u^*, v^*)) &= \text{span}\{\hat{u}_i, \hat{v}_i\}, \end{aligned}$$

here  $(\hat{u}_i, \hat{v}_i) = (1, b_i) \cos \frac{i\pi x}{l}$ , with  $b_i = \frac{d_1 \sigma_i - f_1}{f_2}$ . The accompanying matrix of  $F_{(u,v)}(\xi_i, u^*, v^*)$  is:

$$F_{(u,v)}^*(\xi_i, u^*, v^*) = \begin{pmatrix} d_1 \Delta + f_1 & g_1 - \xi_i \chi(v^*) \Delta \\ f_2 & d_2 \Delta + g_2 \end{pmatrix}.$$

It is easy to see that

$$\mathcal{N}(F_{(\xi_i, u, v)}^*(u^*, v^*)) = \text{span}\{(\hat{u}_i^*, \hat{v}_i^*)\},$$

where  $(\hat{u}_i^*, \hat{v}_i^*) = (1, b_i^*) \cos \frac{i\pi x}{l}$ , with  $b_i^* = -\frac{f_2}{g_2 - d_2 \sigma_i}$ . Thus

$$\dim \mathcal{N}(F_{(u,v)}^*(\xi_i, u^*, v^*)) = 1,$$

and by the Fredholm alternative theorem (see Appendix D of [7]), we obtain

$$\mathcal{R}(F_{(u,v)}(\xi_i, u^*, v^*)) = [\mathcal{N}(F_{(u,v)}^*(\xi_i, u^*, v^*))]^\perp,$$

that is

$$\dim \mathcal{Y} / \mathcal{R}(F_{(u,v)}(\xi_i, u^*, v^*)) = \dim \mathcal{N}(F_{(u,v)}^*(\xi_i, u^*, v^*)) = 1.$$

From the inner product,

$$\begin{aligned} (F_{(\xi, u, v)}(\xi_i, u^*, v^*)(\hat{u}_i, \hat{v}_i), (\hat{u}_i^*, \hat{v}_i^*)) &= - \int_0^1 \sigma_i \chi(v^*) b_i^* \cos^2 \frac{i\pi x}{l} dx \\ &= \frac{\chi(v^*) \sigma_i l f_2}{2(g_2 - d_2 \sigma_i)} > 0. \end{aligned}$$

Then  $F_{(\xi, u, v)}(\xi_i, u^*, v^*)(\hat{u}_i, \hat{v}_i) \notin \mathcal{R}(F_{(u,v)}(\xi_i, u^*, v^*))$ .  $\square$

**Remark 3.2.** According to Theorem 3.1, each  $(\xi_i, u^*, v^*)$  represents a bifurcation point, that is, system (3.1) has infinite bifurcation points. And the emergence of nontrivial steady-state bifurcation solutions is explained by the effect of prey-taxis sensitivity coefficient  $\xi$ .

**Remark 3.3.** The bifurcation curve  $\Gamma_i(s)$ ,  $|s| < \delta$  is part of a connected component  $\Gamma_i$  of  $\bar{S}$  where

$$S = \{(\xi, u, v) \in \mathbb{R} \times \mathcal{X} : F(\xi, u, v) = 0, (u, v) \neq (u^*, v^*)\}.$$

Moreover,  $\Gamma_i$  can be characterised by eigenfunction  $\cos(\frac{i\pi x}{l})$ , when it is around  $(\xi_i, u^*, v^*)$ .

**3.2. Stability of nonconstant steady states.** In this subsection, we investigate the stability of the steady-state solution and provide criterion and explicit formulas to determine the bifurcating direction by employing classical results from [5].

From assumption (H1),  $F$  is  $C^3$ -smooth, and  $(u_i(s, x), v_i(s, x))$  are  $C^3$ -smooth functions of  $s$  by Theorem 1.18 in [4], then we can expand them as follows:

$$\begin{aligned} u_i(s, x) &= u^* + s \cos \frac{i\pi x}{l} + s^2 \Phi_1 + s^3 \Phi_2 + o(s^3), \\ v_i(s, x) &= v^* + sb_i \cos \frac{i\pi x}{l} + s^2 \Psi_1 + s^3 \Psi_2 + o(s^3), \end{aligned} \quad (3.7)$$

where  $(\Phi_k, \Psi_k) \in \mathcal{Z}$ ,  $k = 1, 2$  as defined in Theorem 3.1. Moreover, from the Taylor's expansion, we have

$$\begin{aligned} &\chi(v_i(s, x)) \\ &= \chi(v^*) + s\chi'(v^*)b_i \cos \frac{i\pi x}{l} + s^2(\chi'(v^*)\Psi_1 + \frac{1}{2}\chi''(v^*)b_i^2 \cos^2 \frac{i\pi x}{l}) + o(s^3). \end{aligned} \quad (3.8)$$

For the branch direction of  $\Gamma_i(s)$ , we have the following Lemma.

**Lemma 3.4.** *Suppose that the conditions of Theorem 3.1 are satisfied. Then for each  $i \in \mathbb{N}^+$ ,  $K_1 = 0$  implies the local bifurcation branch  $\Gamma_i(s)$ ,  $|s| < \delta$  is of pitch-fork type, where  $K_1$  is given by (3.3).*

*Proof.* Let

$$\begin{aligned} M_1 &= \frac{1}{2} [f_{uu}(u^*, v^*) + 2f_{uv}(u^*, v^*)b_i + f_{vv}(u^*, v^*)b_i^2], \\ M_2 &= \frac{1}{2} [g_{uu}(u^*, v^*) + 2g_{uv}(u^*, v^*)b_i + g_{vv}(u^*, v^*)b_i^2], \end{aligned}$$

To calculate the value of  $K_1$ , we substitute (3.3), (3.7), and (3.8) into (3.1) and collect the coefficients of the  $s^2$ -terms, then we have

$$\begin{aligned} d_1\Phi_1'' + f_1\Phi_1 + f_2\Psi_1 &= -M_1 \cos^2 \frac{i\pi x}{l}, \\ d_2\Psi_1'' - \xi_i\chi(v^*)\Phi_1'' + g_1\Phi_1 + g_2\Psi_1 + K_1\left(\frac{i\pi}{l}\right)^2\chi(v^*)\cos \frac{i\pi x}{l} &= \quad (3.9) \\ &= -\xi_i\left(\frac{i\pi}{l}\right)^2b_i\chi(v^*)\cos \frac{2i\pi x}{l} - M_2 \cos^2 \frac{i\pi x}{l}. \end{aligned}$$

Multiplying both sides of the first equation of (3.9) by  $\cos \frac{i\pi x}{l}$  and then integrating it over 0 to  $l$ , we obtain

$$\left(f_1 - d_1\left(\frac{i\pi}{l}\right)^2\right) \int_0^1 \Phi_1 \cos \frac{i\pi x}{l} dx + f_2 \int_0^1 \Psi_1 \cos \frac{i\pi x}{l} dx = 0. \quad (3.10)$$

On the other hand, because  $(\Phi_1, \Psi_1) \in \mathcal{Z}$ , we have

$$\int_0^1 \Phi_1 \cos \frac{i\pi x}{l} dx + b_i \int_0^1 \Psi_1 \cos \frac{i\pi x}{l} dx = 0. \quad (3.11)$$

From (3.10) and (3.11), the determinant of the coefficient matrix is

$$\det \begin{pmatrix} f_1 - d_1\left(\frac{i\pi}{l}\right)^2 & f_2 \\ 1 & b_i \end{pmatrix} = -f_2(1 + b_i^2) \neq 0.$$

Therefore, the coefficient matrix is not singular, and we have

$$\int_0^1 \Phi_1 \cos \frac{i\pi x}{l} dx = \int_0^1 \Psi_1 \cos \frac{i\pi x}{l} dx = 0, \quad \forall i \in \mathbb{N}^+. \quad (3.12)$$

Then  $K_1 = 0$  based on the second equation of (3.9) and (3.12). Thus, the local bifurcation branch  $\Gamma_i(s)$ ,  $|s| < \delta$  is of pitch-fork type.  $\square$

We next evaluate  $K_2$  to determine the bifurcation direction and the stability of  $\Gamma_i(s)$ ,  $|s| < \delta$ . To simplify the calculation, we introduce the following notation:

$$\begin{aligned} M_3 &= f_{uu}(u^*, v^*) + f_{uv}(u^*, v^*)b_i, & M_4 &= f_{uv}(u^*, v^*) + f_{vv}(u^*, v^*)b_i, \\ M_5 &= g_{uu}(u^*, v^*) + g_{uv}(u^*, v^*)b_i, & M_6 &= g_{uv}(u^*, v^*) + g_{vv}(u^*, v^*)b_i, \\ M_7 &= \frac{1}{6}(f_{uuu}(u^*, v^*) + 3f_{uuv}(u^*, v^*)b_i + 3f_{uvv}(u^*, v^*)b_i^2 + f_{vvv}(u^*, v^*)b_i^3), \\ M_8 &= \frac{1}{6}(g_{uuu}(u^*, v^*) + 3g_{uuv}(u^*, v^*)b_i + 3g_{uvv}(u^*, v^*)b_i^2 + g_{vvv}(u^*, v^*)b_i^3). \end{aligned}$$

Integrating the equations of system (3.9) over 0 to  $l$  and combining  $K_1 = 0$ , we obtain

$$\int_0^1 \Phi_1 dx = \frac{l(M_2 f_2 - M_1 g_2)}{2(f_1 g_2 - f_2 g_1)}, \quad \int_0^1 \Psi_1 dx = \frac{l(M_1 g_1 - M_2 f_1)}{2(f_1 g_2 - f_2 g_1)}. \quad (3.13)$$

Multiplying the equations of system (3.9) by  $\cos \frac{2i\pi x}{l}$  and then integrating them over 0 to  $l$ , once again combining  $K_1 = 0$  yields

$$\int_0^1 \Phi_1 \cos \frac{2i\pi x}{l} dx = \frac{E_1}{E_0}, \quad \int_0^1 \Psi_1 \cos \frac{2i\pi x}{l} dx = \frac{E_2}{E_0}, \quad (3.14)$$

where

$$\begin{aligned} E_0 &= f_1 g_2 - f_2 g_1 - \frac{4i^2 \pi^2 (\xi_i \chi(v^*) f_2 + g_2 d_1 + f_1 d_2)}{l^2} + \frac{16i^4 \pi^4 d_1 d_2}{l^4}, \\ E_1 &= \frac{\pi^2 i^2 (\xi_i b_i \chi(v^*) f_2 + 2M_1 d_2)}{2l} + \frac{(M_2 f_2 - M_1 g_2)l}{4}, \\ E_2 &= \frac{\pi^2 i^2 (2\xi_i \chi(v^*) M_1 - \xi_i b_i \chi(v^*) f_1 + 2M_2 d_1)}{2l} + \frac{2\pi^4 i^4 \xi_i b_i \chi(v^*) d_1}{l^3} \\ &\quad + \frac{(M_1 g_1 - M_2 f_1)l}{4}, \end{aligned}$$

obviously,  $E_0$  is always nonzero by  $\xi_i \neq \xi_k$  for any  $k \neq i$ .

Substituting (3.7), (3.8) into (3.1), we equate  $s^3$ -terms of (3.1),

$$\begin{aligned} d_1 \Phi_2'' + f_1 \Phi_2 + f_2 \Psi_2 &= -M_3 \Phi_1 \cos \frac{i\pi x}{l} - M_4 \Psi_1 \cos \frac{i\pi x}{l} - M_7 \cos^3 \frac{i\pi x}{l}, \\ d_2 \Psi_2'' - \xi_i \chi(v^*) \Phi_2'' + g_1 \Phi_2 + g_2 \Psi_2 + K_2 \chi(v^*) \left(\frac{i\pi}{l}\right)^2 \cos \frac{i\pi x}{l} \\ &= \xi_i N - M_5 \Phi_1 \cos \frac{i\pi x}{l} - M_6 \Psi_1 \cos \frac{i\pi x}{l} - M_8 \cos^3 \frac{i\pi x}{l}, \end{aligned} \quad (3.15)$$

where

$$\begin{aligned} N &= -\chi'(v^*) \left(\frac{i\pi}{l}\right) \sin \frac{i\pi x}{l} (b_i \Phi_1' + \Psi_1') + \chi'(v^*) \cos \frac{i\pi x}{l} (b_i \Phi_1'' - \left(\frac{i\pi}{l}\right)^2 \Psi_1) \\ &\quad + \chi''(v^*) b_i^2 \left(\frac{i\pi}{l}\right)^2 \cos \frac{i\pi x}{l} \left(\sin^2 \frac{i\pi x}{l} - \frac{1}{2} \cos^2 \frac{i\pi x}{l}\right). \end{aligned}$$

Following  $(\Phi_2, \Psi_2) \in \mathcal{Z}$  and the first equation of system (3.15), we have

$$\begin{aligned} \int_0^1 \Phi_2 \cos \frac{i\pi x}{l} dx &= -b_i \int_0^1 \Psi_2 \cos \frac{i\pi x}{l} dx, \\ \int_0^1 \Psi_2 \cos \frac{i\pi x}{l} dx &= -\frac{1}{(1+b_i^2)f_2} \left[ \frac{M_3}{2} \left( \int_0^1 \Phi_1 dx + \int_0^1 \Phi_1 \cos \frac{2i\pi x}{l} dx \right) \right. \\ &\quad \left. + \frac{M_4}{2} \left( \int_0^1 \Psi_1 dx + \int_0^1 \Psi_1 \cos \frac{2i\pi x}{l} dx \right) + \frac{3M_7 l}{8} \right]. \end{aligned}$$

By the second equation of system (3.15), we have

$$\begin{aligned} K_2 &= -\frac{l}{(i\pi)^2 \chi(v^*)} \left( A_1 \int_0^1 \Phi_2 \cos \frac{i\pi x}{l} dx + A_2 \int_0^1 \Psi_2 \cos \frac{i\pi x}{l} dx \right. \\ &\quad \left. + A_3 \int_0^1 \Phi_1 \cos \frac{2i\pi x}{l} dx + A_4 \int_0^1 \Psi_1 \cos \frac{2i\pi x}{l} dx \right. \\ &\quad \left. + M_5 \int_0^1 \Phi_1 dx + A_6 \int_0^1 \Psi_1 dx + A_7 \right), \end{aligned} \tag{3.16}$$

where

$$\begin{aligned} A_1 &= 2(\xi_i \chi(v^*) (\frac{i\pi}{l})^2 + g_1), & A_2 &= 2(-d_2 (\frac{i\pi}{l})^2 + g_2), \\ A_3 &= M_5 + 2\xi_i \chi'(v^*) b_i (\frac{i\pi}{l})^2, & A_4 &= M_6 - \xi_i \chi'(v^*) (\frac{i\pi}{l})^2, \\ A_6 &= M_6 + \xi_i \chi'(v^*) (\frac{i\pi}{l})^2, & A_7 &= \frac{3M_8 l}{4} + \xi_i \chi''(v^*) \frac{b_i^2 i^2 \pi^2}{8l}. \end{aligned}$$

Therefore, we can evaluate  $K_2$  in terms of system parameters. For the stability of the local bifurcating solution  $\Gamma_i(s)$ , we have the following theorem.

**Theorem 3.5.** *Assuming that the conditions of Theorem 3.1 are satisfied. Let  $K_2$  be given in (3.16),  $i_0$  be a non-negative integer such that  $\xi_{i_0} = \hat{\xi}$  defined by (2.4). Then we have*

- (i) for each  $i \neq i_0$ ,  $\Gamma_i(s)$ ,  $|s| < \delta$  is unstable;
- (ii)  $\Gamma_{i_0}(s)$ ,  $|s| < \delta$  is stable if  $K_2 < 0$  and it is unstable if  $K_2 > 0$ .

*Proof.* (i) Linearizing (3.1) around  $(\xi_i(s), u_i(s, x), v_i(s, x))$ , we obtain the eigenvalue problem

$$F_{(u,v)}(\xi_i(s), u_i(s, x), v_i(s, x))(u, v) = \rho(s)(u, v), \quad (u, v) \in \mathcal{X}. \tag{3.17}$$

When  $s \rightarrow 0$ , (3.17) can be written as

$$F_{(u,v)}(\xi_i, u^*, v^*)(u, v) = \rho(0)(u, v), \tag{3.18}$$

By (2.4) and (2.7), we have

$$Q_i(\sigma_i, \xi_j) = f_2 \chi(v^*) \sigma_i (\xi_i - \xi_j), \quad 0 \leq i, j < \infty.$$

Indeed, if  $j \neq i_0$ , then  $Q_{i_0}(\sigma_{i_0}, \xi_j) < 0$ , which implies (3.18) has a simple eigenvalue  $\rho(0) > 0$  by (3.2). Based on the standard eigenvalue perturbation theory in [14], for smaller  $s$ , there exists a positive real part of the eigenvalue  $\rho(s)$  in the linearized system (3.17). Thus the solution curve  $\Gamma_i(s)$ ,  $|s| < \delta$ ,  $i \neq i_0$  is unstable, which means there must be  $i = i_0$  when the solution curve  $\Gamma_i(s)$ ,  $|s| < \delta$  is stable.

The proof of (ii) is the same as [39, Theorem 4.2], we omit it here. □

It follows from the Remark 3.3, Lemma 3.4, and Theorem 3.5 that the bifurcation curve  $\Gamma_i$  around  $(\xi_i, u^*, v^*)$  is pitch-fork and the stability of the critical local bifurcation branch  $\Gamma_{i_0}(s)$ ,  $|s| < \delta$  depends on  $K_2$ . If  $\Gamma_i(s)$ ,  $|s| < \delta$  is stable, then it must be the right most one on the  $\xi$ -axis, and turns to the left at  $(\xi_i, u^*, v^*)$ .

**3.3. Global bifurcation analysis.** In this subsection, we apply the bifurcation theory in [23] to illustrate the global structure of the bifurcation curve  $\Gamma_i$ , which contains  $(\xi_i, u^*, v^*)$ , and present the following theorem to show that the local solution bifurcation can be extended to a global one.

**Theorem 3.6.** *Assuming that the conditions of Theorem 3.1 are satisfied and  $\sigma_i \neq \frac{c}{d_2}$ , the projection of bifurcation branch  $\Gamma_i$  on the  $\xi$ -axis is  $(-\infty, \xi_i)$ . Furthermore, when  $\xi \neq \xi_i$  for any positive integer  $i$  and  $\xi < \hat{\xi}$ , system (3.1) has at least one nonconstant positive solution.*

*Proof.* By the transformation  $(U, V) = (u - u^*, v - v^*)$ , system (3.1) becomes

$$\begin{aligned} d_1 U'' + (U + u^*)(1 - (U + u^*)) - \frac{(U + u^*)^2(V + v^*)}{a(U + u^*)^2 + (U + u^*) + g} &= 0 \quad x \in (0, l), \\ d_2 V'' - \xi(\chi(V + v^*)U')' + c(V + v^*)(1 - \frac{V + v^*}{\delta(U + u^*)}) &= 0 \quad x \in (0, l), \\ U'(x) = V'(x) = 0 \quad x = 0, l. \end{aligned}$$

We denote

$$H(\xi, U, V) = \begin{pmatrix} d_1 U'' + (U + u^*)(1 - (U + u^*)) - \frac{(U + u^*)^2(V + v^*)}{a(U + u^*)^2 + (U + u^*) + g} \\ d_2 V'' - \xi(\chi(V + v^*)U')' + c(V + v^*)(1 - \frac{V + v^*}{\delta(U + u^*)}) \end{pmatrix}.$$

Let  $w = (p, q) \in \mathcal{X}$ . Then we obtain

$$H_{(u,v)}(\xi, U, V)w = H_1 w'' + H_2(\xi, w, w') = 0,$$

where  $\chi'(V + v^*)$  denotes the derivative of  $\chi(V + v^*)$  with respect to  $V$ ,

$$\begin{aligned} H_1 &= \begin{pmatrix} d_1 & 0 \\ -\xi\chi(V + v^*) & d_2 \end{pmatrix}, \\ H_2(\xi, w, w') &= \begin{pmatrix} h_1 \\ -\xi(\chi(V + v^*)p' + \chi'(V + v^*)(U + u^*)'q) + h_2 \end{pmatrix}, \\ h_1 &= \left[ 1 - 2(U + u^*) - \frac{(U + u^*)(U + u^* + 2g)(V + v^*)}{(a(U + u^*)^2 + (U + u^*) + g)^2} \right] p \\ &\quad - \frac{(U + u^*)^2}{a(U + u^*)^2 + (U + u^*) + g} q, \\ h_2 &= \frac{c(V + v^*)^2}{\delta(U + u^*)^2} p + \left( c - \frac{2c(V + v^*)}{\delta(U + u^*)} \right) q. \end{aligned}$$

It can be seen that,  $\text{Trace}(H_1) > 0$  and  $\text{Det}(H_1) > 0$ , then the operator  $H_1$  is elliptic by Definition 2.1 in [23], furthermore, which is strongly elliptic and satisfies the Agmon's condition for all  $\theta \in [-\frac{\pi}{2}, \frac{\pi}{2}]$  by Case 2 of [23, Remark 2.5.5]. Thus the operator  $H_{(u,v)}(\xi, U, V)$  is the Fredholm operator with zero index by [23, Theorem 3.3 and Remark 3.4].

Therefore,  $\Gamma_i$  must satisfy one of the following conditions:

- (1)  $\Gamma_i$  on  $\mathbb{R} \times \mathcal{X}$  is unbounded;

- (2)  $\Gamma_i$  contains a point  $(\bar{\xi}, u^*, v^*)$ , where  $\bar{\xi} \neq \xi_i$ ;
- (3)  $\Gamma_i$  contains a point where  $(\xi; u, v) \in \partial W$ , where  $W = \{(\xi; u, v) \in \mathbb{R} \times \bar{\mathcal{X}} : u > 0, v > 0\}$ ,

with regard to the global bifurcation result [23, Theorem 4.3]. As we know, the positive solution of the system (3.1) bifurcates from  $(\xi, u^*, v^*)$  if and only if  $\xi = \xi_i$ . Therefore, (2) is ruled out.

Evaluating  $F_{(u,v)}(\xi, u, v)$  at  $(1, 0)$ , we obtain

$$F_{(u,v)}(\xi, 1, 0)(p, q) = \begin{pmatrix} d_1 p'' - p - \frac{q}{a+1+g} \\ d_2 q'' + cq \end{pmatrix}.$$

It is easy to know that if the eigenvalues of the elliptic operator with the homogeneous Neumann boundary condition satisfy  $(\frac{i\pi}{L})^2 \neq \frac{c}{d_2}$ ,  $i = 0, 1, 2, \dots$ , then the boundary  $(1, 0)$  is a non-degenerate equilibrium point. Thus (3) does not hold either.

From the Theorem 1.1, it follows that any positive solution  $(u, v)$  of the system (3.1) is bounded in  $L^\infty(\Omega)$ , and satisfies  $(u, v) \in C^{1,\alpha}(\bar{\Omega})$  for  $\alpha \in (0, 1)$ . Then the Sobolev embedding theorem implies that  $(u, v)$  possesses boundedness in the norm of  $\mathcal{X}$ . Thus,  $\Gamma_i$  extends to infinity in  $\xi$ , which projects on the  $\xi$ -axis as  $(-\infty, \xi_i)$ . □

#### 4. NUMERICAL SIMULATIONS

In this section, we present some numerical simulations to illustrate our theoretical results given in the previous sections. Meanwhile, we can find some interesting patterns of striking structures. Based on Volume-filling mechanism, that is predators stop aggregating after their density attains certain threshold values  $v_m$  and  $\chi(v)$  vanishes identically when  $v \geq v_m$  [1, 21], which satisfies the assumption **(H)**. We take

$$\chi(v) := \begin{cases} 1 - \cos(\frac{2\pi v}{v_m}) & 0 \leq v < v_m, \\ 0 & v \geq v_m. \end{cases}$$

as the sensitivity function.

In Figure 1, the parameters of (1.3) are chosen to be  $d_1 = 0.5$ ,  $d_2 = 1$ ,  $a = \frac{2}{3}$ ,  $g = 2.25$ ,  $c = 3$ ,  $\delta = 1.5$ ,  $v_m = 2$ , which satisfy assumption **(H2)**. By a simple computation, we can obtain that the unique positive homogeneous steady state solution is

$$(u^*, v^*) = (0.75, 1.125),$$

which is stable for the corresponding ODE system.

In Figure 2, parameters are the same as those for Figure 1, and we select the initial data as  $(u_0, v_0) = (u^* + 0.01 \cos x, v^* + 0.01 \cos x)$ , which are small perturbations of  $(u^*, v^*)$ . By (2.3) and (2.4), it is easy to find that

$$\hat{\xi} = \max_{1 \leq i \leq +\infty} \xi_i = \xi_5 \approx -15.6163.$$

Then we observe the pattern formation for the density of predator  $v(x, t)$  when  $\xi = -15.61$  and  $-15.62$  (see Figures 2(a) and 2(b)), and confirm that a steady state bifurcation occurs at  $\hat{\xi} \approx -15.6163$ . From Figures 2(a) and 2(c), we find that the homogeneous steady state solution  $(u^*, v^*)$  is stable for any  $\xi > \hat{\xi}$ . Turing instability at  $(u^*, v^*)$  occurs when  $\xi < \hat{\xi}$ , see Figures 2(b) and 2(d). These graphs also support our stability analysis of steady state solution  $(u^*, v^*)$  in Theorem 2.2.

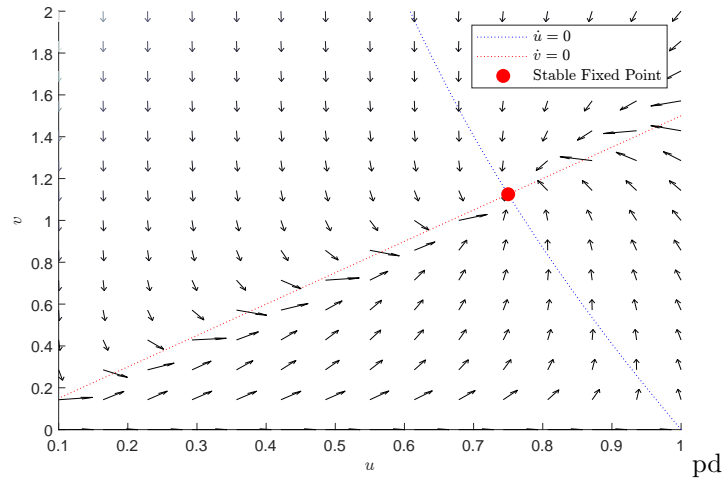


FIGURE 1. Phase diagram.

Moreover, the spatial pattern with mode  $i_0 = 5$  and eigenmode  $\cos \frac{i_0 \pi x}{l} = \cos \frac{\pi x}{2}$  is observed from Figures 2(b) and 2(d).

Figure 3 shows the effect of interval length on the stable wave number, when  $\xi$  is near the critical bifurcation value. System parameters and initial data are taken to be the same as those for Figure 2. Besides, we choose  $l = 13, 21$  and  $29$ , and calculate the corresponding critical bifurcation values of each point to  $\xi_7 \approx -15.6361$ ,  $\xi_{11} \approx -15.6078$ , and  $\xi_{15} \approx -15.6031$ . We observe that the homogeneous steady state solution  $(u^*, v^*)$  loses its stability to the stable wave mode  $\cos \frac{7\pi x}{13}$ ,  $\cos \frac{11\pi x}{21}$  and  $\cos \frac{15\pi x}{29}$ , respectively. Therefore, Theorem 3.5 is verified numerically in Figure 3. Moreover, as the length of interval is increases, the number of aggregates in the spatial pattern become greater and the time for the system to arrive at a non-constant steady state increases.

Figure 4 depicts how a small prey-taxis sensitivity coefficient  $\xi$  affects pattern formation in system (1.3). Here the parameter values and initial values are still chosen in the same way as in Figure 2. Choosing  $l = 15$ , and different prey-taxis sensitivity coefficients:  $\xi = -20$ ,  $\xi = -50$  and  $\xi = -100$ , which are less than the maximum critical bifurcation value  $\xi_8 = -15.6235$ . we can get that  $v(x, t)$  develop into spike functions when the prey-taxis sensitivity coefficient is small. This validates the fact that a small prey-taxis sensitivity coefficient benefits heterogeneity and aggregation of population species in (1.3).

We present a list of plots in Figure 5 to show that a variety of nonconstant steady state solutions, spatio-temporal periodic solutions and spatio-temporal irregular solutions are observed for system (1.3) as the interval length is increased when the prey-taxis sensitivity coefficient  $\xi$  is much smaller than the critical bifurcation value. The system parameters are taken as  $d_1 = 0.5$ ,  $d_2 = 1$ ,  $a = 1$ ,  $g = 0.7125$ ,  $c = 0.9$ ,  $\delta = 0.9$ ,  $v_m = 2$ . We take initial values  $(u_0, v_0) = (u^* + 0.05 \cos x, v^* + 0.05 \cos x)$  and fix  $\xi = -30$ , which is obviously far away from the critical bifurcation value. It is clear that the solution can evolve through a series of emerging and merging. Here merging refers to the combination of two aggregates into one via chemotactic attraction, while emerging refers to the appearance of new aggregation peaks in the

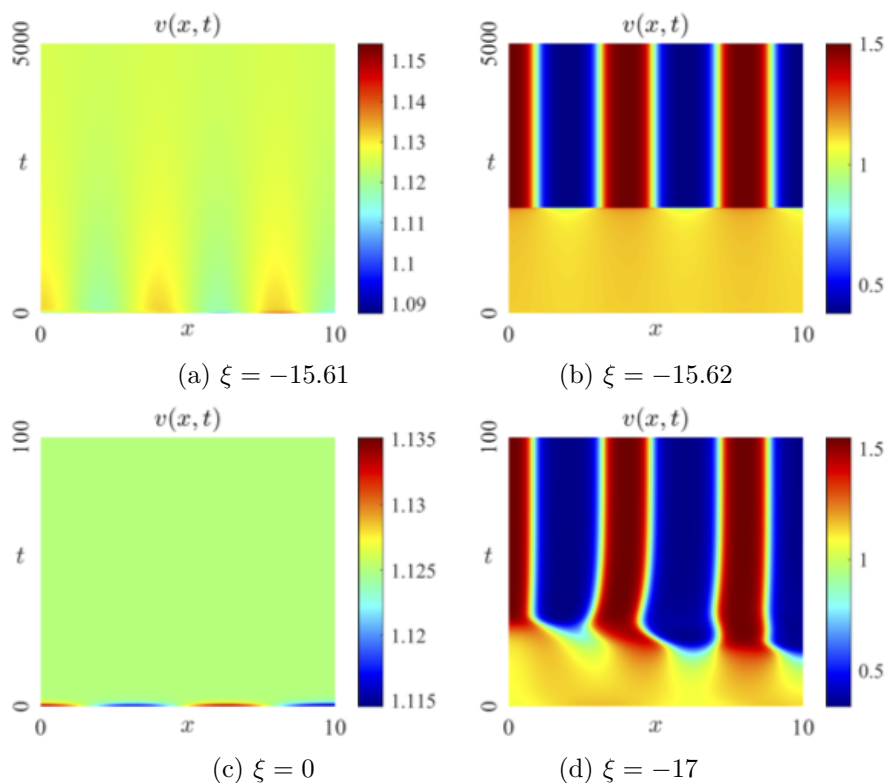


FIGURE 2. Numerical simulation of  $v(x, t)$  of (1.3) over  $l = (0, 10)$ . Here  $d_1 = 0.5$ ,  $d_2 = 1$ ,  $a = 2/3$ ,  $g = 2.25$ ,  $c = 3$ ,  $\delta = 1.5$  with the initial data  $(u_0, v_0) = (u^* + 0.01 * \cos(x), v^* + 0.01 * \cos(x))$ , and  $\xi$  is a variable coefficient. Solutions are plotted for (i) (ii):  $t \in [0, 5000]$ , (iii) (iv):  $t \in [0, 100]$ .

space created by the merger. Except that, the spatio-temporal behavior of the internal spike transfer to the boundary can also be observed. These numerical results reflect the coexistence of predator-prey species and the complexity of the spatio-temporal structure of prey-taxis systems. For the relevant theoretical analysis we can refer to [22].

3021

In Figure 6, system parameter are chosen to be the same as those for Figure 5, except that  $\xi \in [-30.2, -29.5]$ , which are smaller than the critical bifurcation value  $\xi_8 = 6.0879$ . We find that the pattern formation is complex and extremely sensitive to the prey-taxis sensitivity coefficient  $\xi$ . In particular, the dynamics are same initially, while they vary significantly from  $t \approx 200$ , transitioning between regular and irregular patterning.

Finally, we find an interesting phenomenon, that is the intrinsic growth rate of predators  $c$  can influence spatio-temporal periodicity when  $\xi$  is far away from the critical bifurcation value. We take  $d_1 = 0.5$ ,  $d_2 = 1$ ,  $a = \frac{2}{3}$ ,  $g = 2.25$ ,  $\delta = 1.5$  and  $l = 4$ ,  $\xi = -40$  in (1.3). The initial values are the same as Figure 5. It can be seen directly from Figure 7 that there is a corresponding transition from nonconstant

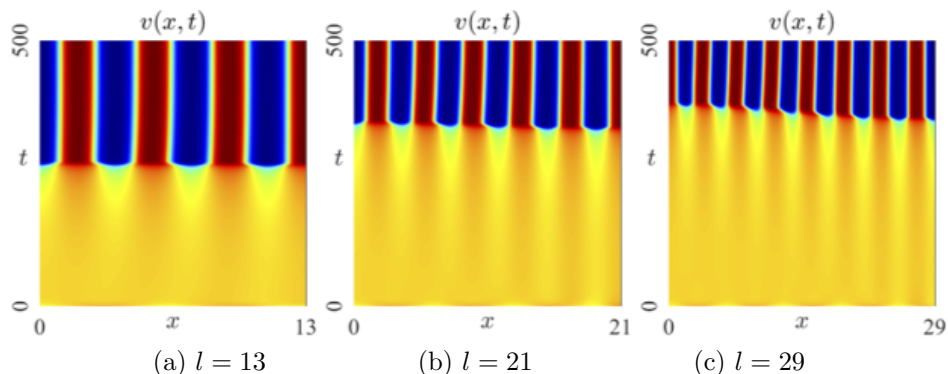


FIGURE 3. Pattern formations of  $v(x, t)$  of (1.3) illustrate the effect of interval length on the stable wave number with  $\xi$  near the critical bifurcation values. System parameters and initial data are the same as in Figure 2.

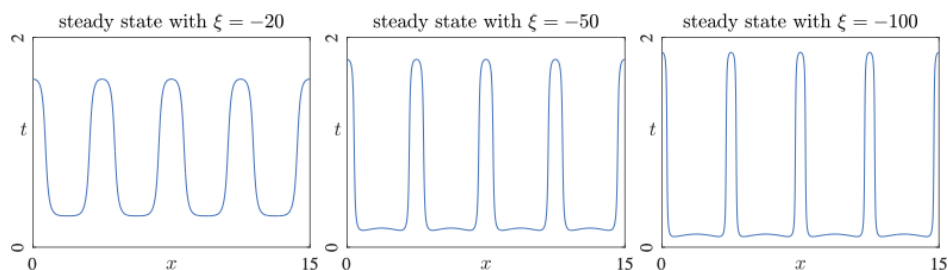


FIGURE 4. Nonconstant steady state solutions of the system (1.3) over  $l = (0, 15)$  show how a small prey-taxis sensitivity coefficient  $\xi$  affects pattern formations. System parameters and initial data are the same as in Figure 2.

steady state solutions to spatio-temporal periodic solutions as  $c$  increases from 2.823 to 2.824. As  $c$  increases from 2.824 to 2.925, we can observe the period of the spatio-temporal periodic solutions becomes greater. And spatio-temporal periodic solutions transform into nonconstant steady state solutions, when  $c$  increases from 3.005 to 3.006. We can suppose that the period becomes infinite in this process. Our numerical simulations indicate that the intrinsic growth rate of predator  $c$  affects the period of sustained coexistence of prey and predator species in the habitat, which enriches the spatial-temporal patterns of the prey-taxis system.

## 5. CONCLUSIONS AND DISCUSSION

In this article, we investigated the dynamics of predator-prey model of Leslie-Gower type with Sigmoid functional response and prey-taxis under the homogeneous Neumann boundary condition. First the global existence of classical solutions is established. Choosing the prey-taxis sensitivity coefficient  $\xi$  as the bifurcation parameter, we establish conditions for Turing pattern formation using linear stability analysis. The existence of nonconstant positive steady state is derived from the local bifurcation theory, and it is proved to be of pitch-fork type. Moreover, we

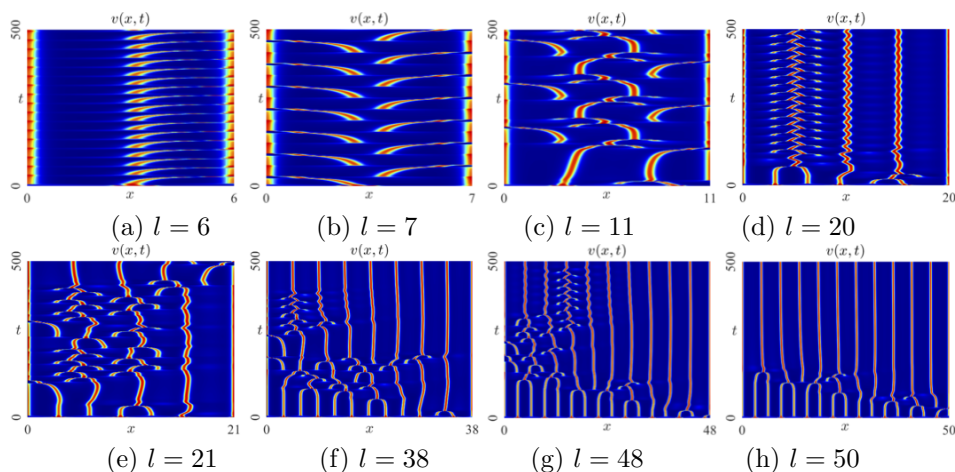


FIGURE 5. A variety of pattern formations are observed as the interval length is increased. System parameters of (1.3) are given as  $(d_1, d_2, a, g, c, \delta) = (0.5, 1, 1, 0.7125, 0.9, 0.9)$  and  $\xi = -30$ .

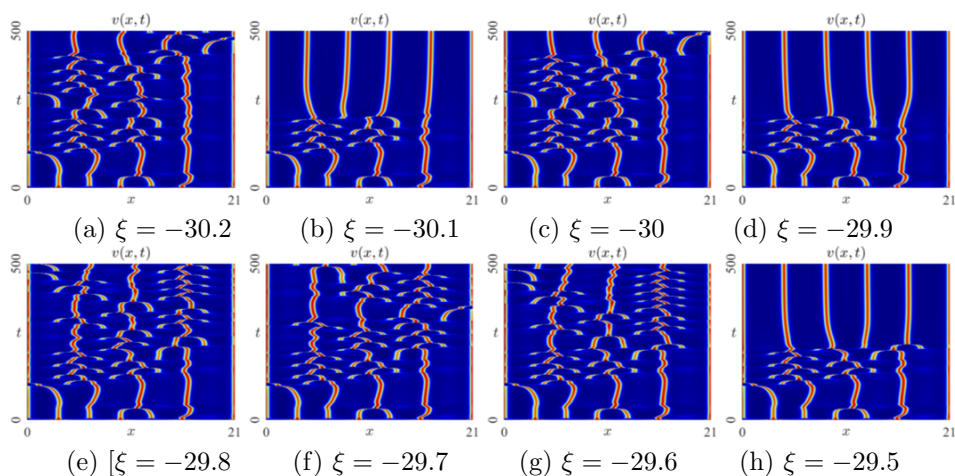


FIGURE 6. Transitions between regular and irregular patterning in (1.3) when  $\xi \in [-30.2, -29.5]$  is far away from the critical bifurcation value. System parameter are chosen to be the same as those for Figure 5.

also obtain formulas to determine the turning and stability of the local bifurcation branch  $\Gamma_i(s)$ . In addition, we show that the bifurcation curves can be extended by applying the global bifurcation theory. Numerical simulations are provided to illustrate and validate our theoretical results. Our findings also reveal that pattern formation is affected by interval length, prey-taxis sensitivity coefficient  $\xi$  and the intrinsic growth rate of predator  $c$  in (1.3).

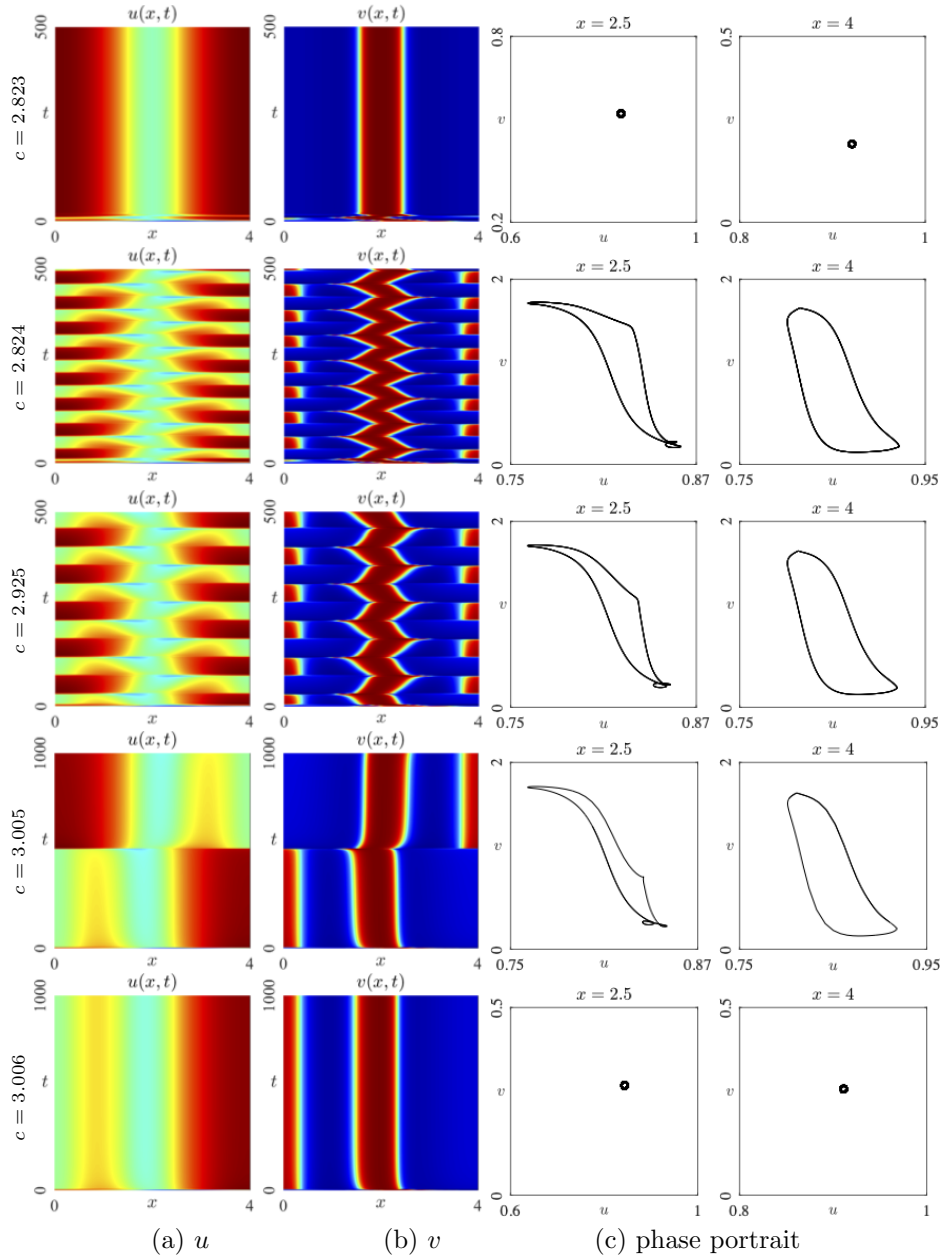


FIGURE 7. Maps of solutions for the system (1.3) show how a variable coefficient  $c$  affects pattern formations for the parameter sets  $(d_1, d_2, a, g, \delta, l, \xi) = (0.5, 1, 2/3, 2.25, 1.5, 4, -40)$  and initial condition sets  $(u_0, v_0) = (u^* + 0.05 \cos x, v^* + 0.05 \cos x)$ . Phase portrait are plotted for  $t \in [100, 2000]$ .

Particularly, when  $\xi$  is away from critical bifurcation value, we can observe nonconstant steady state solutions, spatio-temporal periodic solutions and spatio-temporal irregular solutions as the length interval increases. It is worth noting that solutions evolve to a spatio-temporal pattern with clear temporal periodicity, that is phase plane trajectory gives a closed orbit when  $c$  increases from 2.823 to 2.834. The period of spatio-temporal pattern becomes greater as  $c$  increases from 2.824 to 2.925. And the period tends to infinity as  $c$  tends to 3.006, that is the spatio-temporal pattern backs to a nonconstant steady state solution. But the mathematical behavior of the this process is not well understood yet. We speculate that the effect of the intrinsic growth rate of predators in the pattern formation of the predator-prey model is prevalent, which is worthwhile to explore.

**Acknowledgments.** The authors are grateful to the anonymous referees for their helpful comments and valuable suggestions which have improved the presentation of the manuscript.

#### REFERENCES

- [1] B. Ainseba, M. Bendahmane, A. Noussair; A reaction-diffusion system modeling predator-prey with prey-taxis, *Nonlinear Anal. Real World Appl.*, **9** (2008), no. 5, 2086–2105.
- [2] N. Bellomo, A. Bellouquid, Y. Tao, M. Winkler; Toward a mathematical theory of keller-segel models of pattern formation in biological tissues, *Math. Models Methods Appl. Sci.*, **25** (2015), no. 9, 1663–1763.
- [3] J. Cao, H. Sun, P. Hao, P. Wang; Bifurcation and Turing instability for a predator-prey model with nonlinear reaction cross-diffusion, *Appl. Math. Model.*, **89** (2021), 1663–1677.
- [4] M. G. Crandall, P. H. Rabinowitz; Bifurcation from simple eigenvalues, *J. Functional Analysis*, **8** (1971), 321–340.
- [5] M. G. Crandall, P. H. Rabinowitz; Bifurcation, perturbation of simple eigenvalues and linearized stability, *Arch. Rational Mech. Anal.*, **52** (1973), 161–180.
- [6] B. D. Dalziel, E. Thomann, J. Medlock, P. De Leenheer; Global analysis of a predator-prey model with variable predator search rate, *J. Math. Biol.*, **81** (2020), no. 1, 159–183.
- [7] L. C. Evans; Partial differential equations, vol. 19, *American Mathematical Soc.*, 2010.
- [8] M. P. Hassell, J. H. Lawton, J. R. Beddington; Sigmoid functional responses by invertebrate predators and parasitoids, *J. Anim. Ecol.*, (1977), 249–262.
- [9] X. He, S. Zheng; Global boundedness of solutions in a reaction-diffusion system of predator-prey model with prey-taxis, *Appl. Math. Lett.*, **49** (2015), 73–77.
- [10] G. Hu, X. Li, Y. Wang; Pattern formation and spatiotemporal chaos in a reaction-diffusion predator-prey system, *Nonlinear Dynam.*, **81** (2015), no. 1-2, 265–275.
- [11] J. Huang, S. Ruan, J. Song; Bifurcations in a predator-prey system of Leslie type with generalized Holling type III functional response, *J. Differential Equations*, **257** (2014), no. 6, 1721–1752.
- [12] J. Jorné; Negative ionic cross diffusion coefficients in electrolytic solutions, *J. Theor. Biol.*, **55** (1975), no. 2, 529–532.
- [13] P. Kareiva, G. Odell; Swarms of predators exhibit “preytaxis” if individual predators use area-restricted search, *Am. Nat.*, **130** (1987), no. 2, 233–270.
- [14] T. Kato; Perturbation theory for linear operators, *Classics in Mathematics*, Springer-Verlag, Berlin, 1995, Reprint of the 1980 edition.
- [15] R. Kubo, A. Ugajin, M. Ono; Molecular phylogenetic analysis of mermithid nematodes (mermithida: Mermithidae) discovered from japanese bumblebee (hymenoptera: Bombinae) and behavioral observation of an infected bumblebee, *Appl. Entomol. Zool.*, **51** (2016), no. 4, 549–554.
- [16] J. M. Lee, T. Hillen, M. A. Lewis; Pattern formation in prey-taxis systems, *J. Biol. Dyn.*, **3** (2009), no. 6, 551–573.
- [17] P. H. Leslie; Some further notes on the use of matrices in population mathematics, *Biometrika*, **35** (1948), 213–245.

- [18] P. H. Leslie, J. C. Gower; The properties of a stochastic model for the predator-prey type of interaction between two species, *Biometrika* **47** (1960), 219–234.
- [19] J. D. Murray; Mathematical biology. I, third ed., Interdisciplinary *Applied Mathematics*, vol. 17, Springer-Verlag, New York, 2002, An introduction.
- [20] W. Ni, M. Tang; Turing patterns in the Lengyel-Epstein system for the CIMA reaction, *Trans. Amer. Math. Soc.*, **357** (2005), no. 10, 3953–3969.
- [21] K. J. Painter, T. Hillen; Volume-filling and quorum-sensing in models for chemosensitive movement, *Can. Appl. Math. Q.*, **10** (2002), no. 4, 501–543.
- [22] K. J. Painter, T. Hillen; Spatio-temporal chaos in a chemotaxis model, *Physica D*, **240** (2011), no. 4-5, 363–375.
- [23] J. Shi, X. Wang; On global bifurcation for quasilinear elliptic systems on bounded domains, *J. Differential Equations*, **246** (2009), no. 7, 2788–2812.
- [24] Y. Song, X. Tang; Stability, steady-state bifurcations, and Turing patterns in a predator-prey model with herd behavior and prey-taxis, *Stud. Appl. Math.*, **139** (2017), no. 3, 371–404.
- [25] X. Tang, Y. Song; Bifurcation analysis and turing instability in a diffusive predator-prey model with herd behavior and hyperbolic mortality, *Chaos Solitons Fractals*, **81** (2015), no. part A, 303–314.
- [26] X. Tang, Y. Song; Stability, hopf bifurcations and spatial patterns in a delayed diffusive predator-prey model with herd behavior, *Appl. Math. Comput.* **254** (2015), 375–391.
- [27] Y. Tao; Global existence of classical solutions to a predator-prey model with nonlinear prey-taxis, *Nonlinear Anal. Real World Appl.*, **11** (2010), no. 3, 2056–2064.
- [28] C. Tian, Z. Ling, Z. Lin; Turing pattern formation in a predator-prey-mutualist system, *Nonlinear Anal. Real World Appl.*, **12** (2011), no. 6, 3224–3237.
- [29] A. M. Turing; The chemical basis of morphogenesis, *Philos. Trans. Roy. Soc. London Ser. B*, **237** (1952), no. 641, 37–72.
- [30] R. K. Upadhyay, A. Patra, B. Dubey, N. K. Thakur; A predator-prey interaction model with self-and cross-diffusion in aquatic systems, *J. Biol. Syst.* **22** (2014), no. 04, 691–712.
- [31] J. Wang, J. Wei, J. Shi; Global bifurcation analysis and pattern formation in homogeneous diffusive predator-prey systems, *J. Differential Equations*, **260** (2016), no. 4, 3495–3523.
- [32] M. Wang; Stability and Hopf bifurcation for a prey-predator model with prey-stage structure and diffusion, *Math. Biosci.*, **212** (2008), no. 2, 149–160.
- [33] Q. Wang, Y. Song, L. Shao; Nonconstant positive steady states and pattern formation of 1D prey-taxis systems, *J. Nonlinear Sci.*, **27** (2017), no. 1, 71–97.
- [34] X. Wang, W. Wang, G. Zhang; Global bifurcation of solutions for a predator-prey model with prey-taxis, *Math. Methods Appl. Sci.*, **38** (2015), no. 3, 431–443.
- [35] H. F. Weinberger; Invariant sets for weakly coupled parabolic and elliptic systems, *Rend. Mat.*, (6) **8** (1975), 295–310.
- [36] S. Wu, J. Shi, B. Wu; Global existence of solutions and uniform persistence of a diffusive predator-prey model with prey-taxis, *J. Differential Equations*, **260** (2016), no. 7, 5847–5874.
- [37] S. Wu, J. Wang, J. Shi; Dynamics and pattern formation of a diffusive predator-prey model with predator-taxis, *Math. Models Methods Appl. Sci.* **28** (2018), no. 11, 2275–2312.
- [38] L. Zhang, S. Fu; Global bifurcation for a holling-tanner predator-prey model with prey-taxis, *Nonlinear Anal. Real World Appl.*, **47** (2019), 460–472.
- [39] T. Zhang, X. Liu, X. Meng, T. Zhang; Spatio-temporal dynamics near the steady state of a planktonic system, *Comput. Math. Appl.*, **75** (2018), no. 12, 4490–4504.

ZHIHONG ZHAO

SCHOOL OF MATHEMATICS AND PHYSICS, UNIVERSITY OF SCIENCE & TECHNOLOGY BEIJING, BEIJING 100083, CHINA

*Email address:* zzh@ustb.edu.cn

HUANQIN HU

SCHOOL OF MATHEMATICS AND PHYSICS, UNIVERSITY OF SCIENCE & TECHNOLOGY BEIJING, BEIJING 100083, CHINA

*Email address:* bjkjdxhh@163.com